# INTEGRATION OF DIGITAL IMAGE MATCHING AND MULTI IMAGE SHAPE FROM SHADING

C. Heipke

Chair for Photogrammetry and Remote Sensing
Technical University Munich
Arcisstr. 21, D-8000 Munich 2, Germany
Tel: +49-89-2105 2671; Fax: +49-89-280 95 73; Telex: 522854 tumue d
E-mail: heipke@photo.verm.tu-muenchen.de

Commission III

**ABSTRACT:**

Classical shape from shading (SFS) is based on the analysis of the intensity values of a single digital image in order to derive three dimensional information of the depicted scene. It involves the orthographic projection for the transformation from object to image space and has been successfully applied to weakly textured images. In general the illumination conditions must be known, Lambertian reflection and constant albedo must be assumed for the object surface, and only surface slopes can be determined. Digital image matching for photogrammetric processing on the other hand needs at least two images of the same scene taken from different view points and the images must be well textured. Therefore, the two methods are complementary to each other, and a combined model should yield better results than any of the two separate ones.

In this paper a new global approach is presented integrating digital image matching and multi image SFS in object space. In a least squares adjustment the unknowns (geometric and radiometric parameters of the object surface) are estimated from the pixel intensity values and control information. The perspective projection is used for the transformation from object to image space.

The approach is investigated using synthetic images. The main results of this study are the following:

- Heights of a digital terrain model (DTM) or a digital surface model (DSM) instead of surface slopes can be calculated directly using multi image SFS alone or the combined approach (in this paper the term "DTM" denotes a classical DTM as well as a DSM).
- There is no need for conjugate points in the multi image SFS approach. This is especially important, since in weakly textured images the correspondence problem is extremely hard to solve due to the lack of large image intensity gradients.
- If variable albedo is present in parts of the object surface only the combined approach yields correct results. Multi image SFS and digital image matching alone fail in this case.

**Key Words:** digital photogrammetry, shape from shading, image matching, image analysis, DTM/DSM, theory

## 1. INTRODUCTION

One of the main difficulties of digital photogrammetry presents the automatic measurement of image coordinates of conjugate points for the computation of object space coordinates. This problem is referred to as "digital image matching". It has been a focus of research for nearly thirty years. Early work goes back to Sharp et al. /1965/. During the years many algorithms have been suggested for this task. The state-of-the-art of digital image matching is the use of a global, multi image, object based approach incorporating a hierarchical procedure to provide initial values for the unknown parameters. While feature based matching is faster and seems to be more robust, least squares matching has been found to be more accurate. However, it can be observed, that all algorithms, regardless of their origin in detail, heavily rely on the presence of image texture. In the absence of sufficient image intensity gradients, every matching algorithm will fail to produce correct results.

The rarity of high resolution stereoscopic images of planetary surfaces as well as research in computer vision

have prompted interest in developing algorithms for translating single digital images into three dimensional information of the object surface. These algorithms directly relate an image intensity value to the inclination of the corresponding surface patch relative to the direction of illumination. Such methods are called 'shape from shading' or 'photoclinometry' and have been pioneered by Rindfleisch /1966/ and Horn /1970/. While photoclinometry has been developed for astro-geological research and most applications deal with the reconstruction of planetary terrain profiles /e.g. Davis, Sonderblom 1984/, SFS is a research direction within computer vision and focuses on the reconstruction of surfaces /Horn, Brooks 1989/. Both methods are referred to together in this paper and are abbreviated with SFS. As a consequence of being extremely sensitive to changes in inclination, SFS can detect small terrain undulations that are far below the sensitivity of photogrammetry. On the other hand, SFS relies on the correctness of various assumptions concerning the illumination and the light reflection of the object surface. Furthermore, in classical SFS, only surface slopes instead of heights can be derived. A collection of papers on this topic and an excellent bibliography are contained in Horn, Brooks /1989/.

Since the requirements for digital imagery, in order to be used for digital image matching or for SFS, are more or less complementary to each other, a combination of the two methods should yield reliable results also in image regions, where one of the two methods employed independently fails. Such a combination was already suggested by Barnard, Fischler /1982/. It is also in line with the 'cooperative methods paradigm' of computer vision /McKeown 1991/, which basically states that the combined use of different methods for the same aim improves the results. In this context it is interesting to note that SFS also has its role in the human capability of depth perception. Following the work of Julesz /1971/ and Marr /1982/ it was commonly believed that humans rely only on image features, especially on zero crossings of the second derivative of the image intensity function, for binocular depth perception. Only recently it was shown that binocular SFS alone provides unambiguous depth clues as well /Mallot 1991/.

In this paper a new global approach is presented and investigated integrating digital image matching and multi image SFS in object space. In a least squares adjustment the unknowns (geometric and radiometric parameters of the object surface) are estimated from the pixel intensity values and control information. The perspective projection is used for the transformation from object to image space. Chapter 2 describes a simple model for the generation of a digital image. In chapter 3 a multi image object based least squares matching approach developed over the last years is shortly reviewed. Chapter 4 contains an introduction to SFS. In chapter 5 the integration of digital image matching and multi image SFS is presented. Experimental results using synthetic images are contained in chapter 6. In the last chapter conclusions and an outlook for further research are given.

## 2. A SIMPLE MODEL FOR THE GENERATION OF A DIGITAL IMAGE

In this chapter a model for the generation of a digital image taken with an optical sensor is shortly reviewed, since the resulting equations will be needed in the remaining part of the paper (see Horn /1986/ for more details).

The image irradiance $E_i(x,y)$ at point $P'(x,y)$ in the image plane is formed by light reflected at a point $P(X,Y,Z)$ on the object surface. For this imaging process the well known camera equation (1) holds (for the following derivations see also figure 1):

$$E_i(x,y) = \frac{\pi}{4}\left(\frac{d}{f}\right)^2 \cos^4\alpha \; \tau \; L(X,Y) \qquad (1)$$

| | |
|---|---|
| $x,y$ | image coordinates |
| $X,Y,Z$ | object coordinates |
| $E_i(x,y)$ | image irradiance |
| $d$ | diameter of optical lens |
| $f$ | focal length of optical lens |
| $\alpha$ | angle between optical axis and the ray through P and P' |
| $\tau$ | degree of atmospheric transmission |
| $\bar{v}$ | unit vector in the viewing direction at $P(X,Y,Z)$ |
| $L(X,Y)$ | scene radiance in the viewing direction $\bar{v}$ |

In general, L depends on the illumination (number and size of light sources, direction and radiance of illumination) and on the properties of surface reflection, which in turn depend on the surface material, its microstructu-

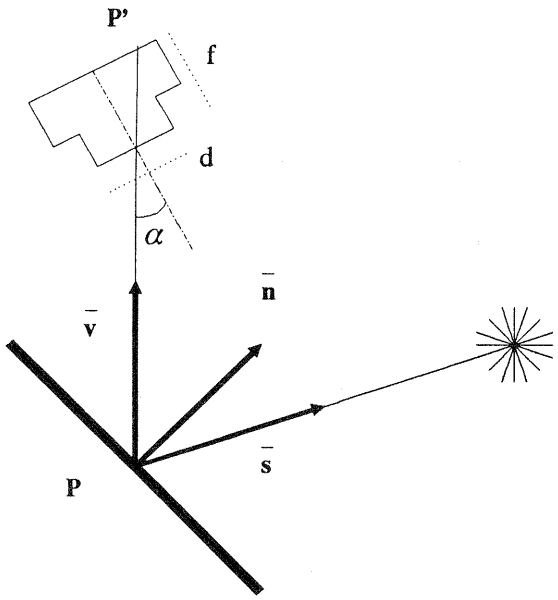


Figure 1: Generation of a digital image

re, the existing moisture and other factors. The surface reflectance properties are normally expressed in the so called bidirectional reflectance distribution function (BRDF).

For reasons of simplicity one distant point light source illuminating the object surface with constant radiance from the direction $\bar{s}$ is introduced only. Also, the object surface is assumed to look equally bright from every viewing direction. This assumption is equivalent to Lambertian reflection, except that light absorption at the object surface is allowed here. The ratio between incoming and reflected radiant flux - a value between 0 and 1 - is called the albedo and is denoted by $\rho(X,Y)$. In this case L can be written as

$$L = \frac{1}{\pi} E_s \rho(X,Y) \frac{\bar{n}\,\bar{s}}{|\bar{n}|} \tag{2}$$

$E_s(X,Y)$ scene irradiance (constant)
$\rho(X,Y)$ albedo of the object surface
$\bar{s}$ unit vector in the direction of illumination at $P(X,Y,Z)$
$\bar{n}$ vector in the direction of the object surface normal at $P(X,Y,Z)$

Combining equations (1) and (2) yields:

$$E_i(x,y) = \frac{\cos^4\alpha}{4} \left(\frac{d}{f}\right)^2 \tau E_s \rho(X,Y) \frac{\bar{n}\,\bar{s}}{|\bar{n}|} \tag{3}$$

In the sensor an image intensity value $g(x,y)$ - in general an integer value between 0 and 255 - is recorded rather than the image irradiance $E_i(x,y)$. $g(x,y)$ is proportional to $E_i(x,y)$:

$$g(x,y) = k\, E_i(x,y) \tag{4}$$

$g(x,y)$ image intensity value at $P'(x,y)$
$k$ rescaling constant

All constants of equations (3) and (4) can be combined with the albedo into the so called object intensity value $G(X,Y)$:

$$G(X,Y) = k \frac{\cos^4\alpha}{4} \left(\frac{d}{f}\right)^2 \tau E_s \rho(X,Y) \tag{5}$$

$G(X,Y)$ object intensity value at $P(X,Y,Z)$

Substituting equations (3) and (5) into (4) yields:

$$g(x,y) = G(X,Y) \frac{\bar{n}\,\bar{s}}{|\bar{n}|} \tag{6}$$

## 3. DIGITAL IMAGE MATCHING

The algorithms for digital image matching are usually classified into three groups:

- image matching using signal processing algorithms (also called area based image matching),
- feature based image matching,
- relational image matching.

In the first group a function of the intensity value differences between selected windows of the different images is minimized. The maximization of the well known cross correlation coefficient /Hannah 1989/ as well as the least squares matching algorithms /Förstner 1982; Grün 1985; Rosenholm 1986/ and phase shift methods /Ehlers 1983/ all belong to this first group. The algorithms of the second group search for predefined features (points, edges, lines, regions) independently in the images /Barnard, Thompson 1980/. Low level image processing algorithms are employed for the selection of the features. Based on the output of these algorithms a list of possibly corresponding features is established. This list still contains a number of gross errors and ambiguities and is thinned out using for instance robust estimation or dynamic programming. The famous zero-crossing algo-

rithm /Marr, Poggio 1979/ is one of the most well known examples of this group, others can be found in Förstner /1986/ and Ackermann, Hahn /1991/. The third group consists of approaches which, besides the features mentioned above, use relations between these features ("parallel to", "to the right of", etc.; for more details see Shapiro, Haralick /1987/ and Boyer, Kak /1988/).

Following the line of thought of chapter 2, equation (6) can be employed to design an object based multi image matching algorithm. This algorithm has been developed as a generalization of the least squares matching methods in the last years /Ebner et al. 1987; Ebner, Heipke 1988/. Similar concepts have been published independently /Wrobel 1987; Helava 1988/. A detailed description of this matching algorithm and an evaluation using synthetic and real imagery can be found in Heipke /1990, 1991/. The outline of this algorithm is shortly reviewed here.

First, a geometric and a radiometric model in object space are introduced.The geometric model consists of a grid DTM. The grid is defined in the XY-plane of the object surface with grid nodes $X_k$, $Y_l$ and grid heights $Z(X_k, Y_l) = Z_{k,l}$. The mesh size depends on the roughness of the terrain. A height $Z(X, Y)$ at an arbitrary point is interpolated from the neighbouring grid heights, e.g. by bilinear interpolation. In the radiometric model object surface elements of constant size are defined within each grid mesh. The size is chosen approximately equal to the pixel size multiplied by the average image scale factor. An object intensity value $G(X, Y)$ is assigned to each object surface element. The albedo $\rho(X, Y)$ of the object surface is allowed to be variable and so is $G(X, Y)$ (see equation (5)). The object surface elements can be projected into the different images using the well known collinearity equations. Subsequently image intensity values at the corresponding locations in pixel space can be resampled from the original pixel intensity values (see also figure 2).

In the following, the grid heights $Z_{k,l}$, the parameters $p$ for the exterior orientation of the images, and the object intensity values $G(X, Y)$ of the object surface elements are treated as unknowns. They are estimated directly from the observations $g(x, y)$ and control information in a least squares adjustment. Thus, $g(x, y)$ depends on $Z_{k,l}$ and on $p$. The surface normal vector $\bar{n}$ is a function of the object surface inclination, and therefore also a

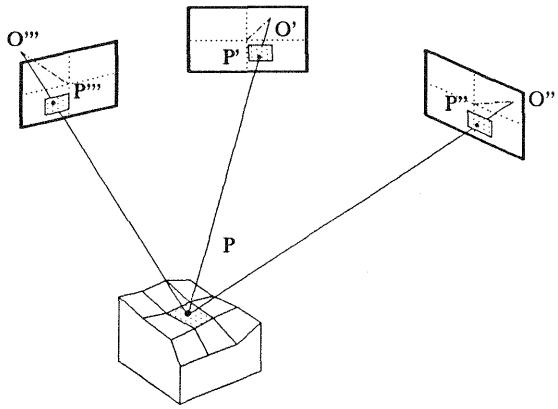


Figure 2: Transformation from object to image space

function of $Z_{k,l}$. The direction of illumination $\bar{s}$ is allowed to vary from image to image. For each object surface element, as many values $g(x, y)$ can be computed as there are images, and as many equations of the following type can be formulated:

$$g_j(x_j(Z_{k,l}, p_j), y_j(Z_{k,l}, p_j)) = G(X, Y)\,\frac{\bar{n}(Z_{k,l})\,\bar{s}_j}{|\bar{n}(Z_{k,l})|} \qquad j = 1, \ldots, n \qquad (7)$$

| | |
|---|---|
| $g_j(x_j(Z_{k,l}, p_j), y_j(Z_{k,l}, p_j))$ | image intensity value, observation from image j |
| $j$ | image index |
| $Z_{k,l}$ | unknown grid heights used to interpolate $Z(X, Y)$ |
| $p_j$ | unknown parameters of exterior orientation of image j |
| $G(X, Y)$ | unknown object intensity value |
| $\bar{n}(Z_{k,l})$ | vector in the direction of the object surface normal |
| $\bar{s}_j$ | unit vector in the direction of illumination for image j |
| $n$ | number of available images |

In optical systems the decreasing image irradiance away from the principal point due to the term $\cos^4\alpha$ (see equations (1), (3) and (5)) is normally compensated for using more than one lens and special coating. Therefore, this effect does not need to be modeled here.

For one object surface element the object intensity value G, and thus the product of all values influencing G (see

equation (5)), must remain constant. In order to partly overcome this limitation, as well as to compensate for surface reflectance properties different from the assumed model, a linear radiometric function accounting for brightness and contrast differences of the various images can be introduced. The resulting system of equations (7) is then completed by adding equations for control information with appropriate standard deviations and rewritten as a system of observation equations. In the most simple case the weight matrix for the intensity value observations is represented by the identity matrix. Since the observation equations are nonlinear in the unknowns, the solution of the least squares adjustment is found iteratively.

## 4. SHAPE FROM SHADING

Classical SFS refers to the problem of reconstructing the surface of an object, given a single digital image by relating the image intensity values directly to surface inclinations relative to the direction of illumination. These inclinations are then integrated to produce a geometric model of the object surface. For the transformation from object to image space the orthographic projection is used. The parameters of exterior orientation are assumed to be known.

The basic equation of SFS is derived from equation (6) by assigning a constant known object intensity value G to the object surface. Looking at equation (5) this is equivalent to assuming a constant known albedo $\rho$, and the other parameters must have calibrated values. Throughout the rest of this paper constant (changing) object intensity values are assumed to result from constant (changing) albedo only.

The surface normal vector $\bar{n}$ can be expressed in terms of the object surface inclination:

$$\bar{n}^T = [\, -\partial Z/\partial X\,,\, -\partial Z/\partial Y\,,\, 1\,] = [\, -Z_X\,,\, -Z_Y\,,\, 1\,] \tag{8}$$

Substituting the unit vector in the direction of illumination as $\bar{s}^T = [s_1\,, s_2\,, s_3\,]$, equation (6) can be written as

$$g(x,y) = G\,\frac{-Z_X\,s_1 - Z_Y\,s_2 + s_3}{\sqrt{Z_X{}^2 + Z_Y{}^2 + 1}} \tag{9}$$

There are two unknowns, namely $Z_X$ and $Z_Y$, but only one observation, namely $g(x,y)$, for each point in object space. Therefore, there exists an infinitive number of solutions to equation (9). This is the fundamental indeterminability of SFS. It can be overcome by working in surface profiles /Horn 1970; Davis, Sonderblom 1984/ or by introducing smoothness terms for the object surface /Strat 1979; Ikeuchi, Horn 1981; Horn, Brooks 1986/.

Some of the rather strong assumptions of SFS can be dropped, if more than one image is used simultaneously. In binocular or in multi image SFS /Grimson 1984/ images taken from different positions are analyzed. The correspondence problem of image matching (there is in general a need for conjugate points) must be overcome. This is particularly complicated for constant albedo due to the lack of intensity gradients. A solution for the estimation of the parameters of exterior orientation is given in de Graaf et al. /1990/.

In the method of photometric stereo /Woodham 1978; Lee, Brady 1991/ images taken from the same position under varying illumination directions are used. Thus, the correspondence problem becomes trivial. Using two images a unique determination of $Z_X$ and $Z_Y$ is possible, the use of three images allows in addition to solve for variable and unknown albedo.

There are also ways to compute object surface heights directly using SFS. Wrobel /1989/ suggests to introduce a discrete geometric model in object space similar to the one described in chapter 3 and to solve for the DTM heights directly. Leclerc, Bobick /1991/ present a solution along the same lines. Horn /1990/ solves for surface inclination and height simultaneously using coupled partial differential equations. An implementation of this approach is described in Szelinski /1991/. Thomas et al. /1991/ investigate an approach combining SFS and stereo radargrammetry to produce DTM from multiple radar images. Kim, Burger /1991/ use a point light source located near the object surface. The resulting variations of the scene irradiance are used to compute surface heights.

## 5. INTEGRATION OF DIGITAL IMAGE MATCHING AND SFS

An algorithm for the synthesis of digital image matching and SFS is presented in this chapter. It combines digital image matching as outlined in chapter 3 and multi image SFS from the previous chapter. Object heights instead of slopes are calculated from two or more images with different illumination in a least squares adjustment. The problem of correspondence is circumvented in this approach.

Looking again at equation (7), but introducing known exterior orientation parameters, the image intensity value $g(x, y)$ can be written as

$$g_j(x_j(Z_{k,l}), y_j(Z_{k,l})) = G(X, Y) \frac{\bar{n}(Z_{k,l})\,\bar{s}_j}{|\bar{n}(Z_{k,l})|} \tag{10}$$

The $Z_{k,l}$ and the object surface intensity $G(X, Y)$ are the only unknowns in equation (10).

If for the whole object surface the assumption of constant albedo is fulfilled, equation (10) describes multi image SFS using the perspective instead of the orthographic projection for the transformation from object to image space. However, it is not necessary to use corresponding points, because all the object surface elements are constrained to lie on the surface defined by the neighbouring grid heights $Z_{k,l}$. This will also be shown experimentally in the next chapter.

If on the other hand variable albedo (texture) is present on the object surface, equation (10) is equivalent to equation (7) and digital image matching as outlined in chapter 3 can be used.

Let us now assume, that it is known a priori which parts of the object surface have constant and which parts have variable albedo. This knowledge can come from image preprocessing or from surface cover information. The related DTM meshes can then be processed accordingly. In equations (11) and (12) A denotes a constant, and $G(X, Y)$ a variable object intensity value. Two groups of observation equations follow:

$$v_j(x_j, y_j) = A \frac{\bar{n}(Z_{k,l})\,\bar{s}_j}{|\bar{n}(Z_{k,l})|} - g_j(x_j(Z_{k,l}), y_j(Z_{k,l})) \tag{11}$$

$v_j(x_j, y_j)$ residual of observation equation resulting from image j

$A$ constant object intensity value

for DTM meshes with constant albedo and

$$v_j(x_j, y_j) = G(X, Y) \frac{\bar{n}(Z_{k,l})\,\bar{s}_j}{|\bar{n}(Z_{k,l})|} - g_j(x_j(Z_{k,l}), y_j(Z_{k,l})) \tag{12}$$

for DTM meshes with variable albedo.

In a least squares adjustment the unknown grid heights $Z_{k,l}$ and the unknown object intensity values A and $G(X, Y)$ can be computed from the observed image intensity values $g(x, y)$. Since the observation equations are nonlinear in the unknowns, the solution must be found iteratively. It should be pointed out that in line with photometric stereo A can only be solved for, if a minimum of three images is used. Otherwise A must be known a priori.

## 6. EXPERIMENTAL RESULTS

Some experimental results for the integration of digital image matching and multi image SFS are presented in this chapter in order to demonstrate the potential of the described approach. They have all been conducted using two synthetic images of a sphere taken from different positions and under different illumination directions. A horizontal plane is introduced as an initial DTM and the sphere is reconstructed from the two images. The idea is to show that multi image SFS yields good results, if the assumption of constant known albedo is correct. If this assumption is violated in parts of the object surface, there are three possibilities to proceed:

- regard the variable unknown albedo in these parts as noise and still use a SFS approach assuming constant known albedo,
- perform digital image matching instead under the wrong assumption, that enough large intensity gradients are present,

- use the combined approach described in the previous chapter.

It is shown that only the last possibility yields correct results under the given circumstances.

### 6.1. Input images

The upper part of a sphere with a radius of 36 m was approximated with a DTM of 64 * 64 meshes by interpolating the grid heights at a mesh size of 1 m from the sphere. From this DTM two shaded relief images were generated using two distant point light sources with identical radiance, illumination directions with equal zenith distance and 90 degrees difference in azimuth, Lambertian reflection, a constant predefined albedo at the object surface, and 8 * 8 object surface elements for each DTM mesh. These images are called OP1 and OP2 respectively. In order to simulate variable albedo for some parts of the object surface, a small number of randomly distributed DTM meshes was chosen and the intensity values inside these meshes were replaced by random noise. The same noise was applied to OP1 and OP2. The two resulting images are called OP3 and OP4. All four images can be seen in figure 3.

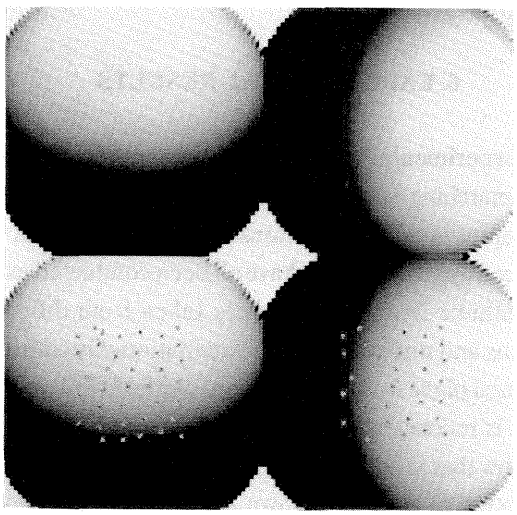

Figure 3: From left to right, top to bottom: OP1 to OP4

Next, two camera stations were defined (for the position of the sphere relative to these stations see figure 4). Using a ray tracing algorithm, OP1 and OP3 were projected into the image plane of station 1, while OP2 and OP4 were projected into that of station 2, always taking the DTM into account for the third dimension. The

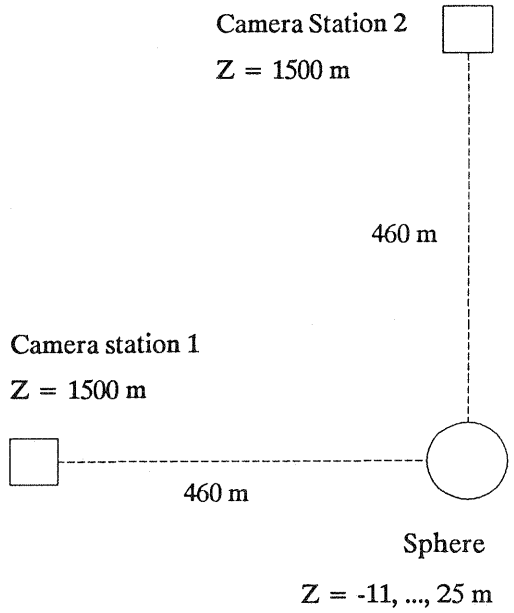


Figure 4: Setup for the generation of IMA 1 to IMA 4

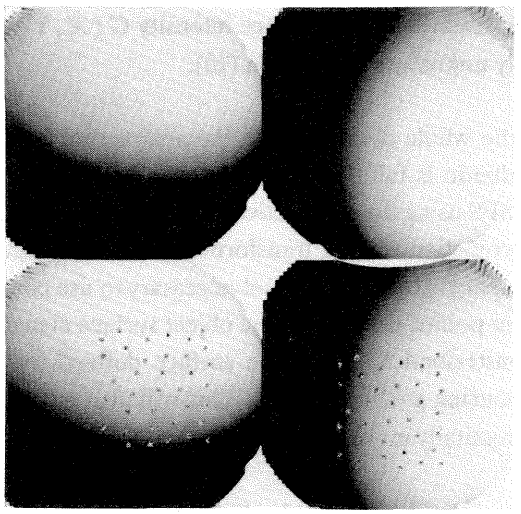

Figure 5: From left to right, top to bottom: IMA1 to IMA4

resulting images are called IMA1, IMA2, IMA3, and IMA4 respectively. They can be seen in figure 5. Thus two sets of synthetic images were generated from the sphere, one set (IMA1 and IMA2) with constant known albedo, the other one (IMA3 and IMA4) with areas of constant known and of variable unknown albedo.

### 6.2. The experiments

A number of experiments has been conducted using two synthetic images at each run. The inner 32 * 32 DTM meshes were processed only in order to avoid occlusions. In the meshes of constant albedo, the known albedo

value was introduced. The directions of illumination used for the creation of the shaded relief images were introduced as constant values, as well as the parameters of exterior orientation chosen for IMA1 to IMA4. A horizontal plane situated tangentially to the sphere was used to provide initial values for the DTM heights. The maximum difference between true and initial height values, which can be found in the corners of the 32 * 32 DTM meshes, amounts to 8 m, equivalent to approximately 20 pixels in image space. All experiments were stopped when the changes to the unknown heights from one iteration to the next fell below a predefined threshold of 0.01 m (0.025 pixels in image space).

The following experiments were conducted:

1) Multi image SFS for the whole object surface with the correct assumption of constant known albedo and the corresponding images IMA1 and IMA2.
2) ditto, but in contrast to experiment 1 without using conjugate points. The object surface elements were alternately projected into IMA1 or IMA2.
3) Multi image SFS for the whole object surface with the assumption of constant known albedo, but using the images IMA3 and IMA4 corrupted by noise.
4) Digital image matching for the whole object surface using the images IMA3 and IMA4 corrupted by noise.
5) The combined approach described in chapter 5 using the images IMA3 and IMA4 corrupted by noise. Correct albedo assumptions (variable unknown albedo for the DTM meshes corrupted by noise, constant known albedo for the rest of the object surface) were introduced.

### 6.3. Results

The results of the 5 experiments can be seen in table 1. The experiment number, the number of iterations for convergence, the mean deviation d and the RMS error $\mu$ of the differences between the computed and the true DTM heights is given. According to the nature of the experiments the shown values should rather be interpreted as trends. They are not meant to be accuracy measures as such.

The following conclusions can be drawn from these results:

| No. of experiment | No. of iterations | d | $\mu$ |
|---|---|---|---|
| - | - | m | m |
| 1 | 20 | 0.01 | 0.02 |
| 2 | 20 | 0.00 | 0.02 |
| 3 | 28 | -1.2 | 1.3 |
| 4 | no convergence | | |
| 5 | 30 | 0.01 | 0.03 |

Table 1: Results of the experiments

- multi image SFS is useful to compute directly height values of the object surface, if the assumption of constant known albedo is correct (experiment 1),
- in this case there is no need for conjugate points, if the described geometric object model is introduced (experiment 2),
- multi image SFS can converge to local minima and produces incorrect results, if variable unknown albedo is present in parts of the object surface (experiment 3),
- in this case digital image matching does not yield correct results either, because the intensity gradients are too small in most meshes (experiment 4),
- if variable unknown albedo is present in parts of the object surface, only using the combined approach a correct result is obtained (experiment 5 as compared to experiments 3 and 4).

## 7. CONCLUSIONS AND OUTLOOK

The presented approach for the integration of digital image matching and multi image SFS in object space has been shown to yield superior results than any of the two methods employed alone. However, only synthetic images have been used, and a number of implicitly or explicitly stated assumptions have to be fulfilled. Also, the question of existence and uniqueness - a wide field of investigation especially in SFS - has not been touched. Therefore, the reported results must be verified, and the approach robustified in order to be used in practical environments.

Some directions for further research shall be pointed out:

- Point light sources near the object rather than far away /Kim, Burger 1991/ or extended light sources can be introduced.

- The direction of illumination does not have to be known, but may be estimated in the least squares adjustment /Leclerc, Bobick 1991/. In the linearisation of equations (11) and (12) the corresponding terms have to be taken into account.
- More than one light source can be present for one image. The scene irradiance is then simply a combination of the individual irradiances.
- A BRDF more complicated than Lambertian reflection can be incorporated /de Graaf et al. 1990/. However, the BRDF must be analytically given.
- Also the parameters of exterior orientation of the images can be considered unknown and can be estimated in the least squares adjustment, if an appropriate BRDF is introduced.
- The sensor must be carefully calibrated in terms of geometric and radiometric distortion.

Other generalisations, for example time variable scene irradiance and BRDF for multi image acquisition, non-opaque object surfaces, occlusions, mutual reflection, and breaklines in the object surface are more difficult to model.

Practical applications of the presented approach are possible in close range and in natural environments. However, care has to be taken for the latter case to ensure that the necessary variations in the direction of illumination can be matched with those available from the sun.

In summary, the combination of photogrammetric algorithms and those from computer vision must be seen as very important in order to automate vision tasks.

## 8. REFERENCES

| | |
|---|---|
| ACSM | American Congress on Surveying and Mapping |
| ASPRS | American Society of Photogrammetry and Remote Sensing |
| BuL | Bildmessung und Luftbildwesen (now Zeitschrift für Photogrammetrie und Fernerkundung) |
| CVGIP | Computer Vision, Graphics and Image Processing |
| DAGM | Deutsche Arbeitsgemeinschaft für Mustererkennung |
| IEEE-PAMI | Institute of Electrical and Electronical Engineers, Transactions on Pattern Analysis and Machine Intelligence |
| IJCV | International Journal of Computer Vision |
| IntArchPhRS | International Archives for Photogrammetry and Remote Sensing |
| PE&RS | Photogrammetric Engineering and Remote Sensing |


Ackermann F., Hahn M., 1991: Image pyramids for digital photogrammetry, in: Ebner H., Fritsch D., Heipke C. (Eds.), Digital Photogrammetric Systems, Wichmann, Karlsruhe, 43-58.

Barnard S.T., Fischler M.A., 1982: Computational stereo, Association for Computing Machinery Computing Surveys (14) 4, 553-571.

Barnard S.T., Thompson W.B., 1980: Disparity analysis of images, IEEE-PAMI (2) 4, 333-340.

Boyer K.L., Kak A.C., 1988: Structural stereopsis for 3-D vision, IEEE-PAMI (10) 2, 144-166.

Davis P.A., Sonderblom L.A., 1984: Modelling crater topography and albedo from monoscopic Viking orbiter images, Journal of Geophysical Research (89), 9449-9457.

Ebner H., Fritsch D., Gillessen W., Heipke C., 1987: Integration von Bildzuordnung und Objektrekonstruktion innerhalb der digitalen Photogrammetrie, BuL (55) 5, 194-203.

Ebner H., Heipke C., 1988: Integration of digital image matching and object surface reconstruction, IntArchPhRS (27) B11, III-534-545.

Ehlers M., 1983: Untersuchungen von digitalen Korrelationsverfahren zur Entzerrung von Fernerkundungsaufnahmen, Wissenschaftliche Arbeiten der Fachrichtung Vermessung der Universität Hannover 121.

Förstner W., 1982: On the geometric precision of digital correlation, IntArchPhRS (24) 3, 176-189.

Förstner W., 1986: A feature based correspondence algorithm for image matching, IntArchPhRS (26) 3/3, 150-166.

de Graaf A.J., Korsten M.J., Houkes Z., 1990: Estimation of position and orientation of objects from stereo images, in: Großkopf R. (Ed.), Mustererkennung 1990, Proceedings, 12. DAGM-Symposium Aalen, Springer, Berlin, 348-355.

Grimson W.E.L., 1984: Binocular shading and visual surface reconstruction, CVGIP (28) 1, 19-43.

Grün A., 1985: Adaptive least squares correlation: a powerful image matching technique, South African Journal of Photogrammetry, Remote Sensing and Cartography (14) 3, 175-187.

Hannah M.J., 1989: A system for digital stereo image matching, PE&RS (55) 12, 1765-1770.

Heipke C., 1990: Integration von digitaler Bildzuordnung, Punktbestimmung, Oberflächenrekonstruktion und Orthoprojektion in der digitalen Photogrammetrie, DGK, Reihe C, 366.

Heipke C., 1991: A global approach for least squares image matching and surface reconstruction in object space, ACSM-ASPRS Auto Carto 10 Annual Convention, Technical Papers (5), 161-171; also in press, PE&RS (58).

Helava U.V., 1988: Object-space least-squares correlation, PE&RS (54) 6, 711-714.

Horn B.K.P., 1970: Shape from shading: a method for obtaining the shape of a smooth opaque object from one view, Ph. D. thesis, Department of Electrical Engineering, MIT.

Horn B.K.P., 1986: Robot Vision, The MIT Press, Cambridge.

Horn B.K.P., 1990: Height and gradient from shading, IJCV (5) 1, 37-75.

Horn B.K.P., Brooks M.J., 1986: The variational approach to shape from shading, CVGIP (33) 2, 174-208.

Horn B.K.P., Brooks M.J. (Eds.), 1989: Shape from shading, The MIT Press, Cambridge.

Ikeuchi K., Horn B.K.P., 1981: Numerical shape from shading and occluding boundaries, Artificial Intelligence (17) 1-3, 141-184.

Julesz B., 1971: Foundation of cyclopean perception, University of Chicago Press, Chicago.

Kim B., Burger P., 1991: Depth and shape from shading using the photometric stereo method, CVGIP - Image Understanding (54) 3, 416-427.

Leclerc Y.G., Bobick A.F., 1991: The direct computation of height from shading, Proceedings, IEEE Computer Society Conference on Computer Vision and Pattern Recognition, 552-558.

Lee S., Brady M., 1991: Integrating stereo and photometric stereo to monitor the development of glaucoma, Image and Vision Computing (9) 1, 39-44.

Mallot H., 1991: Frühe Bildverarbeitung in neuronaler Architektur, in: Radig B. (Ed.), Mustererkennung 1991, Proceedings, 13. DAGM-Symposium München, Springer, Berlin, 19-34.

Marr D., 1982: Vision, Freeman, New York.

Marr D., Poggio T., 1979: A computational theory of human stereo vision, Proceedings of the Royal Society London B. 204, 301-328.

McKeown D.M., 1991: Information fusion in cartographic feature extraction, in: Ebner H., Fritsch D., Heipke C. (Eds.), Digital Photogrammetric Systems, Wichmann, Karlsruhe, 103-110.

Rindfleisch T., 1966: Photometric method for lunar topography, Photogrammetric Engineering (32) 2, 262-277.

Rosenholm D., 1986: Accuracy improvement of digital matching for evaluation of digital terrain models, IntArchPhRS (26) 3/2, 573-587.

Shapiro L.G., Haralick R.M., 1987: Relational matching, Applied Optics (26) 10, 1845-1851.

Sharp J.V., Christensen R.L., Gilman W.L., Schulman F.D., 1965: Automatic map compilation using digital techniques, PE&RS (31) 3, 223-239.

Strat T.M., 1979: A numerical method for shape from shading from single images, S.M. thesis, Department of Electrical Engineering and Computer Science, MIT.

Szelinski R., 1991: Fast shape from shading, CVGIP - Image Understanding (53) 2, 129-153.

Thomas J., Kober W., Leberl F., 1991: Multiple image SAR shape from shading, PE&RS (57) 1, 51-59.

Woodham R.J., 1980: Photometric method for determining surface orientation from multiple images, Optical Engineering (19) 1, 139-144.

Wrobel B., 1987: Digitale Bildzuordnung durch Facetten mit Hilfe von Objektraummodellen, BuL (55) 3, 93-101.

Wrobel B., 1989: Geometrisch-physikalische Grundlagen der digitalen Bildmessung, Schriftenreihe Institut für Photogrammetrie, Universität Stuttgart (13), 223-242.